Electron Microscopic Structural Analysis of Photosystem I, Photosystem II, and the Cytochrome b6/f Complex from Green Plants and Cyanobacteria

Boekema, Egbert J.; Boonstra, Arjen F.; Dekker, Jan P.; Rögner, Matthias

Published in:
Journal of Bioenergetics and Biomembranes

DOI:
10.1007/BF00763217

Publication date:
1994

Journal of Bioenergetics and Biomembranes, Vol. 26, No. 1, 1994

Electron Microscopic Structural Analysis of Photosystem I, Photosystem II, and the Cytochrome *b6/f* Complex from Green Plants and Cyanobacteria

Egbert J. Boekema,[1] Arjen F. Boonstra,[1] Jan P. Dekker,[2] and Matthias Rögner[3]

Received July 27, 1993; accepted October 5, 1993

Electron microscopy (EM) in combination with image analysis is a powerful technique to study protein structure at low- and high resolution. Since electron micrographs of biological objects are very noisy, substantial improvement of image quality can be obtained by averaging individual projections. Crystallographic and noncrystallographic averaging methods are available and have been applied to study projections of the large protein complexes embedded in photosynthetic membranes from cyanobacteria and higher plants. Results of EM on monomeric and trimeric Photosystem I complexes, on monomeric and dimeric Photosystem II complexes, and on the monomeric cytochrome *b6/f* complex are discussed.

KEY WORDS: Photosystem I; Photosystem II; cytochrome *b6/f*; electron microscopy;. subunit arrangement.

INTRODUCTION

The energy-transducing complexes Photosystem I, Photosystem II, cytochrome *b6/f*, and ATP synthase in the thylakoid membrane of chloroplasts and cyanobacteria mediate the conversion of solar energy into chemically fixed energy. They are large membrane-bound supramolecular complexes with an intriguing complexity.

The Photosystem I (PS I) complex catalyzes the light-dependent transfer of electrons from reduced plastocyanin or cytochrome *c*553 to soluble ferredoxin. It is a multi-subunit complex consisting of about 12–14 subunits, depending on the source (Bryant, 1992). For the subunit nomenclature, the gene coding names are becoming the standard. PsaA and PsaB are two large subunits with a mass of about 82–83 kDa. They harbor the primary electron donors and the more primary acceptors. Also they bind most of the antennae chlorophyll molecules. Other subunits, which have been named PsaC through PsaN, all have a mass below 20 kDa and can be found in cyanobacterial and higher-plant PS I, except for PsaG and PsaH, which are only present in higher plants (Ikeuchi, 1992).

The Photosystem II (PS II) complex is also a multi-subunit complex, with at least 17 subunits, including several small ones with a mass under 10 kDa (Erickson and Rochaix, 1992). About 10 subunits are necessary for plastoquinone reduction and oxygen evolution. A complex consisting of the membrane-embedded subunits D1 (PsbA) and D2 (PsbD), the α and β subunits of cytochrome b_{559} (PsbE and PsbF), and the PsbI gene product forms the photochemical reaction center. An extrinsic 33-kDa subunit (PsbO) stabilizes the manganese cluster that catalyzes oxygen evolution. Among the other subunits, the two largest ones have respective masses of 47 and 43 kDa (PsbB and PsbC) and bind chlorophyll *a* molecules. The PS II structure is not known at high resolution. But even at low

[1] BIOSON Research Institute, Biophysical Chemistry, University of Groningen, Nijenborgh 4, 9747 AG Groningen, The Netherlands.
[2] Department of Physics and Astronomy, Institute of Molecular Biology Sciences, Free University, De Boelelaan 1081, 1081 HV Amsterdam, The Netherlands.
[3] Institute of Botany, University of Münster, Schlossgarten 3, D-48149 Münster, Germany.

0145-479X/94/0200-0017$07.00/0

resolution, structural information is scarce. Since all the various subunits have been sequenced, predictions of the polypeptide folding have been made, especially for the D1 and D2 subunits (Svensson *et al.*, 1990) because these two subunits are related to their counterparts from the structurally well-resolved reaction center of purple bacteria. Apart from this, most of the subunit positions and interactions are not exactly known. Models for the subunit positions, based on biochemical experiments, have been presented (Dainese *et al.*, 1992).

The cytochrome *b6/f* complex mediates electron transport between PS II and PS I by oxidizing plastoquinol and reducing plastocyanin or cytochrome *c*553. In comparison to PS I and PS II it is of simpler subunit composition and contains four major subunits (O'keefe, 1988), which are named cytochrome *f* (PetA, 34 kDa), cytochrome *b*6 (PetB, 23 kDa), the Rieske protein (PetC, 20 kDa), and subunit IV (PetD, 17 kDa). One or two subunits with a mass below 10 kDa are also thought to be present (Haley and Bogorad, 1989).

EM is one of the techniques for studying the structure of proteins and membranes. Previously, the main contribution of EM in the field of photosynthesis was the application of freeze-fracture techniques. They give useful information on the overall size and distribution of the complexes embedded in the membranes (Staehelin, 1988). Due to advances in specimen preparation and image analysis methods, EM is also becoming an important tool for the study of the isolated macromolecules of the photosynthetic membranes at more detail. This paper reviews results on PS I, PS II, and the cytochrome *b6/f* complex. The other major membrane-bound complex, ATP synthase, will not be discussed here, since the chloroplast ATP synthase is quite similar to the bacterial and mitochondrial complexes. Their structures were recently reviewed in this journal (Amzel *et al.*, 1992; Capaldi *et al.*, 1992). Information on the membrane-bound part, F_0, is found in Boekema *et al.*, 1988. Structural data on the soluble part, F_1, are summarized in Boekema *et al.* (1992).

STRUCTURE DETERMINATION BY ELECTRON MICROSCOPY

Electron microscopy (EM), in combination with image analysis, is a technique to study macromolecular structures at medium resolution (15–25 Å). In principle, a much higher resolution is possible, because the resolving power of an electron microscope is enough to record images with a resolution of approximately 2–3 Å. However, for different reasons such resolution will not be possible in the case of biological materials. One reason is the low contrast of biomacromolecules. Another important factor is the radiation damage caused by the electron beam. Radiation damage cannot be avoided, but only minimized, by cooling the specimen to liquid-nitrogen or liquid-helium temperature and by minimizing the electron dose. As a result, the electron micrographs are noisy and the object is hardly visible. Therefore image analysis techniques have been developed to improve the signal recorded in the noisy EM pictures. In practice, this is done by averaging over many projections. There are two general methods for averaging, depending on the object. One method is based on filtering images of periodic objects, which are usually two-dimensional crystals; the other deals with single-particle projections.

Projections of single particles can be averaged after they have been brought into equivalent positions by shifting them rotationally and translationally. This aperiodic averaging technique or single-particle analysis is able to reveal the predominant projections of protein molecules (Frank *et al.*, 1988). The fact that crystallization of the protein is not required is an advantage of this method. A disadvantage is that the maximal possible resolution by single-particle analysis is restricted to about 15 Å. This limit is set by the signal-to-noise ratio, which is related to the size of the object and with a relative low value for small objects. This in turn causes inaccuracies in the rotational and translational alignments. The resolution is also limited by the fact that the particles are not restricted to a definite position, as in a crystal. Small deviations from a common position cause slight differences between similar-looking projections, resulting in a resolution of 25 Å or worse for objects smaller than about 200–300 kDa.

Negative staining with metal salts, such as uranyl acetate, is a general technique to improve the contrast and has also been used successfully for membrane proteins (Boekema, 1991). To prepare EM samples with well-resolved single-particle projections, the protein should remain in a monodispersed form until it dries in together with the heavy metal stain. This is achieved by keeping the detergent concentration

above the CMC (critical micellar concentration). In negatively stained specimens of membrane proteins the contrasting agent is not replacing nor contrasting most of the detergent shell. The protein plus its detergent shell is stain-excluding. We noticed that slight irregularities or flexibilities in the detergent are present, causing a slight variance in particle shape and diameter. For the single-particle analysis, this reduces the resolution considerably for the smaller membrane proteins in comparison to water-soluble proteins. For monomeric Photosystem I or Photosystem II (mass about 300 kDa) single-particle analysis is not sufficiently accurate to reveal much of the inner structure; it only gives a good impression of the overall dimensions. For larger particles, like trimeric Photosystem I, the contribution of the detergent boundary layer is relatively smaller and does not limit the resolution of the averaging method. Although single-particle averaging is able to resolve the structure up to 15 Å in favorable cases, this resolution is sufficient for the localization of subunit positions in projections. Examples will be given for Photosystems I and II.

A more precise way to analyze protein structure by EM is to work on two-dimensional crystals. The advantage of an analysis of a periodic object is the much higher signal-to-noise ratio. This enables an accurate determination of the positions of the molecules and thus, in principle, averaging is possible at a resolution of (much) better than 15 Å. For crystals of about 1 μm in size, a resolution of about 15–25 Å is usual. Optimal results can be obtained by the so-called correlation technique. Photosystem I crystals will be shown as an example for the periodic averaging methods. With respect to the resolution that can be obtained, there is not a clear lower limit for the mass of the protein to be crystallized. In fact, smaller proteins (10–50 kDa) are advantageous, because they allow averaging over a larger number of projections.

If two-dimensional crystals with a diameter of at least several micrometers can be grown, EM can be performed with a high resolution. For some small membrane proteins with a mass of 20–40 kDa, averaging over very large areas resulted in a projected structure with a resolution better than 5 Å. For bacteriorhodopsin the three-dimensional structure could be determined entirely from EM data by fitting the amino acid chain into the electron density (Henderson *et al.*, 1990). In the field of photosynthesis, such a high-resolution structure determination of the LHCII complex from pea is almost completed (Kühlbrandt and Wang, 1991). For proteins with a mass between 300 and 600 kDa, like Photosystems I and II and ATP synthase; solving the structure by high-resolution EM would be difficult. The preferential size of two-dimensional crystals of such objects is at least 10–20 μm. However, up to now growing crystals of such a size was not possible.

While a low-resolution structure by single-particle averaging can be obtained within weeks, obtaining a high-resolution structure from EM data may take several years. The limit of a structure determination at high resolution is merely in making large crystals in which the molecules are well ordered. Once this prerequisite is fulfilled, a resolution better than 10 Å is possible. In conclusion, EM techniques are available to study isolated (membrane) protein complexes from very small to very large sizes. In combination with techniques used in cell biology for studying whole cells or cell fragments, EM has the possibility and the potential to come up with a full

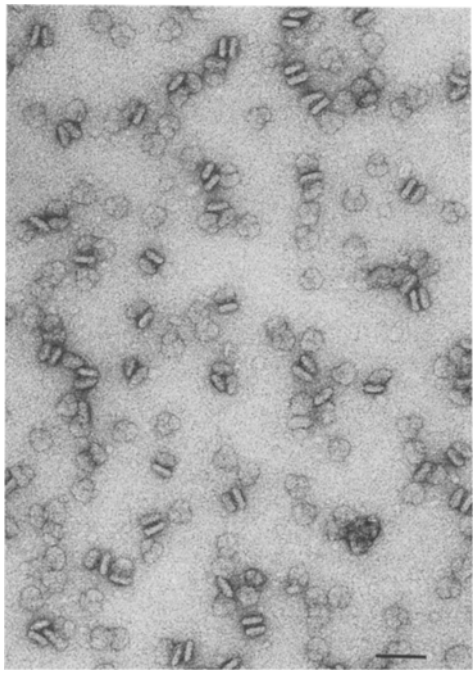

Fig. 1. Electron microscopy of PS I trimeric particles from the cyanobacterium *Synechocystis* PCC 6803. A part of an electron micrograph showing negatively stained PS I particles in top view position (circular views) and side view position (rodlike views). Side views shows that trimers have a tendency to artificially aggregate into pairs with the stromal exposed subunits PsaC, -D, and -E on the inside. The bar represents 500 Å.

picture of the photosynthetic membrane and its interacting proteins.

PHOTOSYSTEM I FROM CYANOBACTERIA

Since 1987 significant progress has been made in the structure elucidation of PS I from cyanobacteria. The first EM studies that were able to reveal the PS I structure dealt with trimeric particles with a diameter of about 200 Å, which were isolated from the thermophilic cyanobacterium *Synechococcus elongatus* (Boekema *et al.*, 1987, 1989). More recently, we also analyzed PS I trimers (P700–F_A/F_B complex) from a mesophilic cyanobacterium, *Synechocystis* PCC 6803 (Kruip *et al.*, 1993). From electron micrographs, such as the one of Fig. 1, we could separate the top-view projections by analysis into two types, which are mirror-related. These two types are generated because particles are asymmetric and can be

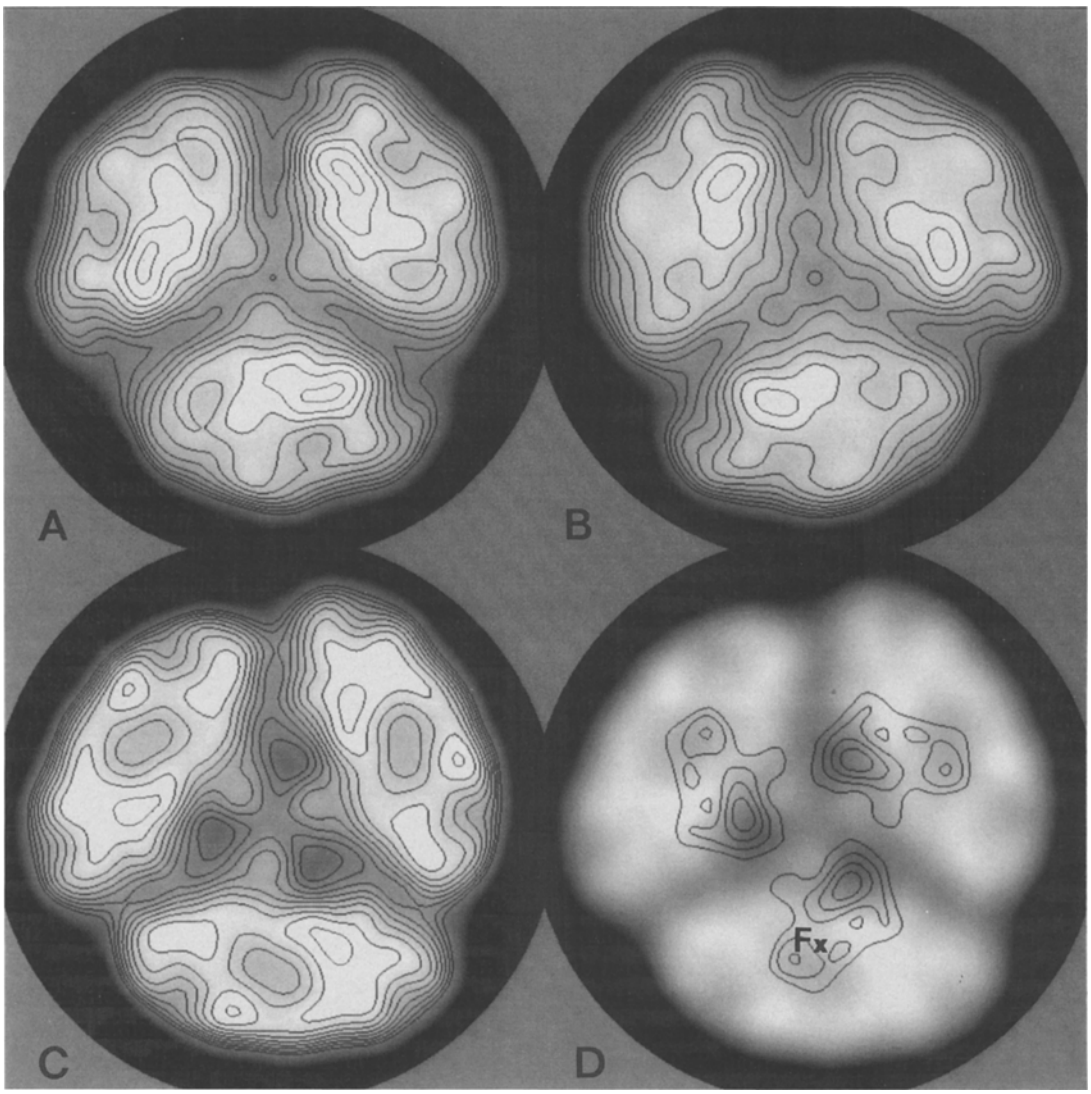

Fig. 2. Final result of single-particle averaging of *Synechocystis* PCC 6803 trimeric PS I projections (modified from Kruip *et al.*, 1993). (A) sum of PS I particles (P700–F_AF_B complex) in "flip" type projection; (B) sum of PS I particles in "flop" type projection; (C) sum of projections from a PS I particle without subunits PsaC, -D, and -E (P700–F_X complex). (D) sum of PS I particle projections on which the difference image between A and C has been imposed. The position of iron-sulfur center F_X, derived from a comparison with the 6 Å X-ray map (Krauss *et al.*, 1993), has been indicated. The diameter of the circular mask is 206 Å.

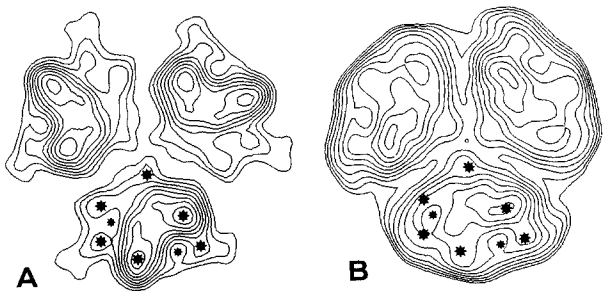

Fig. 3. A comparison of PS I projections from *Synechococcus* and *Synechocystis* PS I. (A) Three monomers from an analysis of two-dimensional crystals from *Synechococcus* PS I (Böttcher *et al.*, 1992) fitted by correlation methods in the equivalent positions of the three monomers in the *Synechocystis* trimers of the sum of Fig. 2A. The image is shown in the contours-only version. In one monomer, local density maxima and minima have been indicated with large and small asterices. (B) The sum of Fig. 5A shown in the contours-only version with the maxima and minima of *Synechocystis* superimposed.

attached to the carbon support film in two ways (upside-up and upside-down or "flip" and "flop"). Figure 2A, B shows the results from the analysis of the *Synechocystis* trimers with improved resolution (15–20 Å) due to optimized preparation conditions (Kruip *et al.*, 1993). The height of the original *Synechococcus elongatus* particles, measured from side views, was only 65 Å (Boekema *et al.*, 1989). This suggests that the first *Synechococcus* trimers had lost small subunits (possibly the extrinsic subunits PsaC, -D, and -E) upon isolation or sample preparation for EM. This idea is confirmed by the finding of thicker (92 Å) PS I particles in later *Synechococcus* preparations (unpublished results). We also analyzed smaller particles from which subunits PsaC, -D, and -E were selectively removed by salt washing, the so-called P700–F_X complex (Kruip *et al.*, 1993). The averaged projection (Fig. 2C) differs substantially from those of PS I with all the subunits present, but resembles the previous projection from *Synechococcus* trimers (Boekema *et al.*, 1989).

PS I has also been crystallized into two-dimensional arrays (Ford *et al.*, 1990; Böttcher *et al.*, 1992). Monomeric PS I from *Synechococcus elongatus* was crystallized by removal of detergent from PS I-enriched membranous material (Fig. 4). Usually crystalline double layers were observed, caused by the collapse of a vesicle crystal, but monolayers were also frequent. The largest crystals measured $0.5 \times 1\ \mu$m in size (Böttcher *et al.*, 1992). For double layers, the images of the two layers could be processed separately (Fig. 5). Features in the two-dimensional projection could be enhanced with a resolution of 15–18 Å. In contrast to the crystals, image analysis on single monomeric PS I only revealed the outer contours (Rögner *et al.*, 1990), yet this was sufficient for a first estimation of the molecular mass of the PS I monomer, i.e., 235 ± 25 kDa, excluding the detergent shell. The three-dimensional appearance of PS I was calculated by combining filtered images of tilted crystals. The model shows an asymmetric PS I

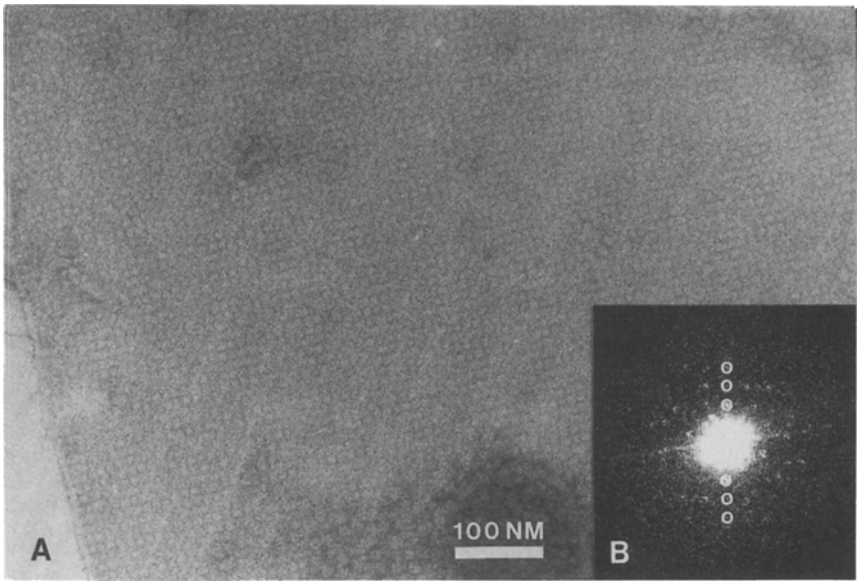

Fig. 4. Part of an electron micrograph showing a collapsed membrane crystal of PS I monomers from *Synechococcus elongatus* (taken from Böttcher *et al.*, 1992, with permission).

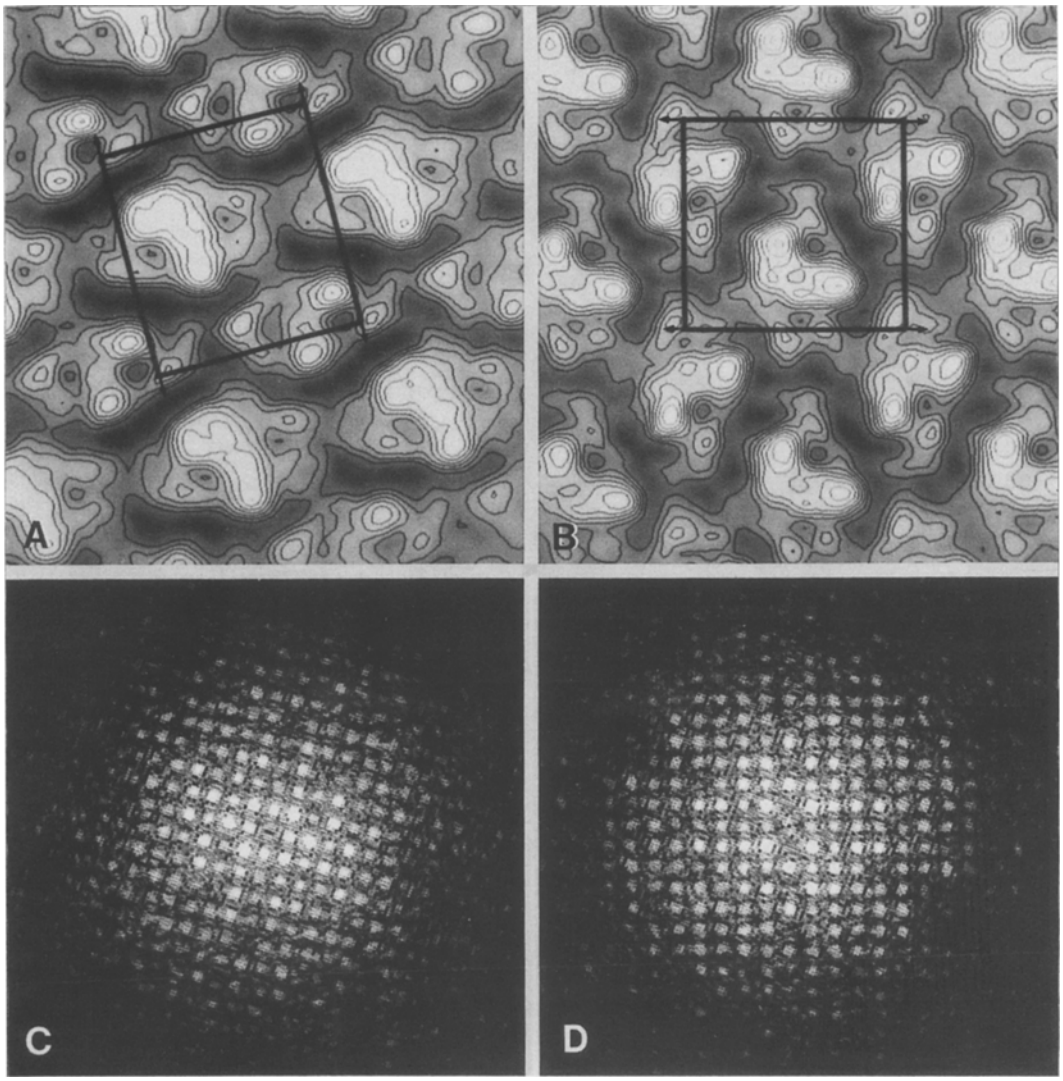

Fig. 5. Image analysis of the two layers of a collapsed vesicle crystal of *Synechococcus* PS I monomers (taken from Böttcher *et al.*, 1992, with permission).

complex (Fig. 6). On one side (presumably the stromal side) there is a 30 Å high ridge. The other side (presumably the lumenal side) is rather flat, but in the center there is a 30 Å deep indentation (Böttcher *et al.*, 1992). A three-dimensional structure of *Synechococcus* PS I at 6 Å, based on X-ray diffraction of three-dimensional crystals, was published more recently (Krauss *et al.*, 1993). The outer contours of the EM reconstruction resemble those of the X-ray structure fairly well. But due to its higher resolution, the latter model reveals more details, such as the position of the three iron-sulfur centers, two of which are known to be attached to subunit PsaC, whereas the third one is shared by subunits PsaA and PsaB. The electron density map at 6 Å resolution does not yet permit, however, fitting in all subunit polypeptide chains, due to which a positioning of the subunits would be possible. Our three-dimensional model derived from two-dimensional crystals has a height of 100 Å (Böttcher *et al.*, 1992), which is 8 Å more than the value determined from the aggregated side views of *Synechocystis* (Kruip *et al.*, 1993). The discrepancy of 8 Å may be due to some interdigitating of trimers upon face-to-face aggregation. The reduction of height in the PS I particles without PsaC–E subunits was found to be 33 Å

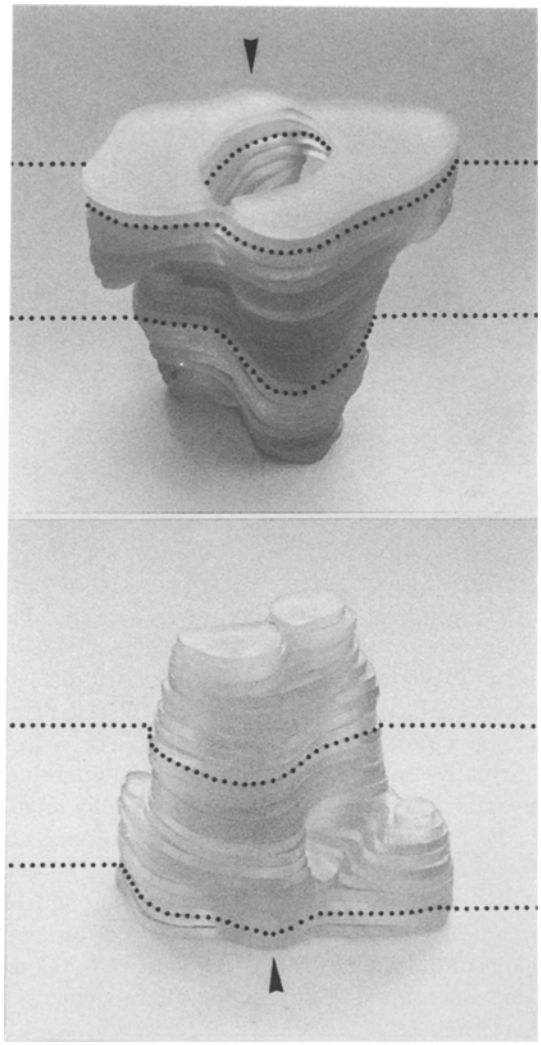

Fig. 6. A low-resolution model for cyanobacterial PS I calculated from tilted two-dimensional crystals (taken from Böttcher *et al.*, 1992, with permission).

(Kruip *et al.*, 1993), which is similar to that of the 35 Å ridge seen in the 6 Å X-ray diffraction model (Krauss *et al.*, 1993). Thus, the EM data indicate that the stroma-exposed ridge is exclusively filled by PsaC, -D, and -E.

Figure 3 compares the top views of PS I particles from *Synechococcus* and *Synechocystis* on the same scale. This figure shows that the outer contours of both images differ substantially. Possibly this is caused mainly by differences in attached lipid and detergent molecules in the boundary layer and by the state of aggregation (monomeric versus trimeric). The PS I monomers from *Synechocystis* are arranged in trimers and have attached dodecyl maltoside on their hydrophobic sides, whereas the monomers from *Synechococcus*, which are single monomers, are mainly surrounded by lipids. The inner features of the monomers, however, appear more similar. Minima and maxima in the staining profile of *Synechococcus* have been indicated by asterisks (Fig. 3A) and their locations have been superimposed on the *Synechocystis* trimer (Fig. 3B). The deviation between 7 equivalent positions in both cyanobacteria is about 5 Å. This indicates a close structural similarity between PS I from both species. On the other hand, the amplitudes (height) of several maxima in *Synechocystis* and *Synechococcus* are not the same; also flip and flop projections are often not fully identical (Fig. 2A and B). The reason for this is the substantial difference in structure of the stromal and the lumenal side of PS I, which is obvious from the 3D model of *Synechococcus* PS I shown in Fig. 6. On the lumenal side of the model there is an indentation, which is superimposed in projection with a ridge on the stromal side. The more the indentation is stain-filled, the smaller the ridge will appear in the projection. This is usually the case if the indentation faces the carbon support film. However, when particles are compared that are embedded in about the same type of stain layer, this problem is minimized (Fig. 2).

We also analyzed trimeric PS I complexes from the prochlorophyte *Prochlorothrix hollandica*, an organism related to the cyanobacteria, but with an antenna system containing chlorophyll *b* (Van der Staay *et al.*, 1993). In comparison to *Synechococcus* and *Synechocystis*, positions of stain-excluding areas were compatible, but the similarities in projected structure were not so striking as between PS I of the latter two cyanobacteria.

To visualize the difference between the flip image of the PS I particles (Fig. 2A) and the PS I particles lacking subunits PsaC–E (Fig. 2C) in projection, the images were subtracted after normalization. The difference image between 2A and 2C was then superimposed on the image of Fig. 2C. Figure 2D shows that only in the center of the monomer are relevant differences present. Thus, PsaC, -D, and -E should be located in this area. On its lumenal side, the model shows a 30 Å deep indentation (Fig. 6), which is oval in shape (Böttcher *et al.*, 1992). This same indentation shows up in the projection of the P700–F_X complex as an oval stain pit (Fig. 2C). As a whole, the image of the P700–F_X complex looks more like the sections of the model on the lumenal side than

the stromal side (Böttcher *et al.*, 1992). The ridge extending from the 3D model on the stromal side coincides largely with the difference area of Fig. 2D, which is not exactly in the center of the monomer, but shifted toward the center of the trimer. Figure 2D also shows that the small knobs in the center of the trimer are similar for both types of images and are close to the contoured difference area. Due to the removal of the subunits PsaC–E, the knobs can be clearly seen in the image of the P700–F_X complex (Fig. 2C). Their separate position, which is also clear from the X-ray map (Krauss *et al.*, 1993), indicates that these knobs are formed by one of the small subunits. Due to the considerable loss of PsaL in monomeric PS I (in comparison to PS I trimers), this subunit is a strong candidate for this position (Kruip *et al.*, 1993). This is in line with recent results showing that PS I particles isolated from a PsaL-less mutant have lost their ability to form trimers (Chitnis *et al.*, 1993).

PHOTOSYSTEM I FROM HIGHER PLANTS

Three types of PS I particles, isolated from spinach, have been characterized by EM (Boekema *et al.*, 1990). The largest particle, PSI-200, contains all the higher-plant PS I subunits, including the light-harvesting antenna complex I (LHCI) polypeptides. The PS-100 particle lacks these LHCIs; it therefore resembles monomeric cyanobacterial PS I, including subunits PsaC–E. The smallest particle, CPI, lacks most of the (extrinsic) subunits and mainly contains the large subunits PsaA and -B. It was found that no precise alignment of EM projections was possible for CPI. However, shape and size at low resolution are similar to monomeric PSI from *Synechococcus*.

The major difference between higher plant PS I and cyanobacterial PS I is the association of LHCI units to PS I in higher plants. Four types of LHCI polypeptides have been found. They were recently named Lhca1 to Lhca4. For the PSI-200 particle, consisting of the PS I core complex and attached LHCI polypeptides, dimensions of 160 × 120 Å in the plane of the membrane were found (Boekema *et al.*, 1990). The difference in shape and size between the PSI-200 (Fig. 7) and the CPI particles in the top view projection is depicted in Fig. 8. This difference should mainly be accommodated by the LHCI's and is most compatible with a number of 8 of such LHCI complexes surrounding PS I in a ringlike configuration as

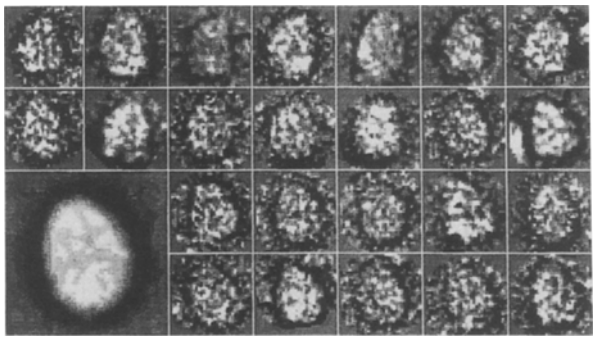

Fig. 7. EM of PS I from spinach. A gallery of single-particle projections from PSI-200 particles and an average image of 104 aligned projections (taken from Boekema *et al.*, 1990, with permission).

shown in Fig. 8. The conclusion that each PSI-200 particle binds about 8 LHCI complexes is in good agreement with stoichiometric calculations that resulted from labeling experiments of the PS I complex from the green alga *Chlamydomonas* (Schuster *et al.*, 1988). Since 8 copies is the most likely number, two copies of each type of polypeptide would be a possibility. However, it has been found that usually one LHCI polypeptide predominates (Schwartz *et al.*, 1991). This makes it highly unlikely that a PS I complex is surrounded by two copies from each of the four different LHCI complexes. To determine the exact stoichiometry of the different LHCI polypeptides, further studies are required. However, they are complicated by the fact that the PSI-200 preparations were found to be slightly inhomogeneous.

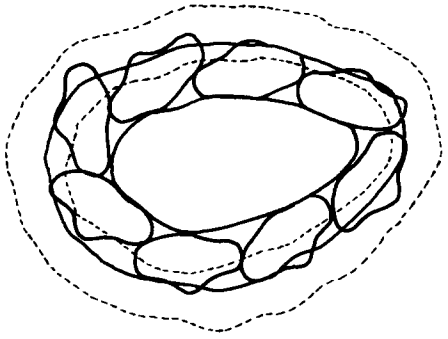

Fig. 8. A tentative model for the LHCI subunit arrangement in the PSI-200 complex from spinach, in which the core complex (PSI-100) is shown as enclosed in a shell of eight LHCI subunits. Dotted lines indicate the contours of the detergent complexes PSI-200 and CPI. Solid lines indicate the contours of both particles after correction for a detergent boundary layer of 17 Å (taken from Boekema *et al.*, 1990, with permission).

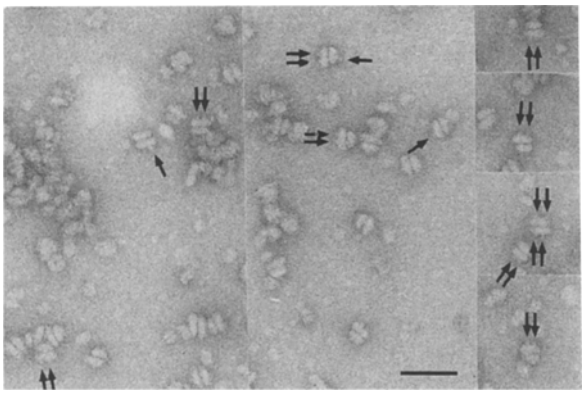

Fig. 9. Six parts of one electron micrograph of negatively stained, isolated PS II dimers from the cyanobacterium *Synechococcus elongatus* (unpublished results). The particles are lying predominantly in side view position and often artificially aggregate into pairs of dimers. The arrows indicate protrusions seen in side-view position; often two protrusions from one dimer are visible. It is thought that they consist of the 33-kDa subunit of the oxygen-evolving complex. Similar protrusions are visible on aggregated spinach PS II monomers (Haag *et al.*, 1990. The bar indicates 500 Å.

PHOTOSYSTEM II FROM CYANOBACTERIA

Our first experiments to investigate the overall shape and dimensions of isolated PS II were performed on monomeric and dimeric particles purified from the thermophilic cyanobacterium *Synechococcus elongatus* (Rögner *et al.*, 1987; Dekker *et al.*, 1988). We visualized these particles in the presence of the detergent dodecyl maltoside by negative staining with uranyl acetate. It was found that in the membrane plane the monomer is about oval in shape with overall dimensions of 123 × 75 Å. The dimeric particle (dimensions of 120 × 155 Å, corrected for detergent) was twice as large as the monomer. The height of these particles vertical to the membrane was determined in two ways. From individual projections we obtained an average height of 64 and 66 Å for the monomer and dimer, respectively. From stacks of aggregated particles the height, expressed as the center-to-center distance (= repeat of the stack), was 76 and 80 Å, respectively (Dekker *et al.*, 1988). The latter way of expressing the height of PS II is more appropriate because it accounts for the maximal height. Images of dimeric PS II from *Synechococcus elongatus*, taken recently with a better resolution, clearly show protrusions in the side view position (Fig. 9). Often two protrusions can be seen on one dimer. The protrusions are thought to represent the 33-kDa oxygen-evolving subunit. As both monomeric and dimeric type of *Synechococcus* PS II particles were highly active in oxygen evolution, this provides strong evidence that each monomer contains a complete set of the subunits essential for oxygen evolution and plastoquinone reduction.

The presence of a detergent boundary layer around the monomeric PS II particles isolated from spinach and cyanobacteria and their relatively small size prevents an accurate image analysis. In principle, PS II dimers would form a better object for image analysis. Averaged top views of dimeric PS II show that the dimers are built up from two monomers which are arranged in an antiparallel way (Fig. 11A, B). Each monomer also has a close-to-dimeric appearance. At lower resolution this results in a tetrameric appearance of PS II on the lumenal side of the membrane, which was also noticed before for PS II in

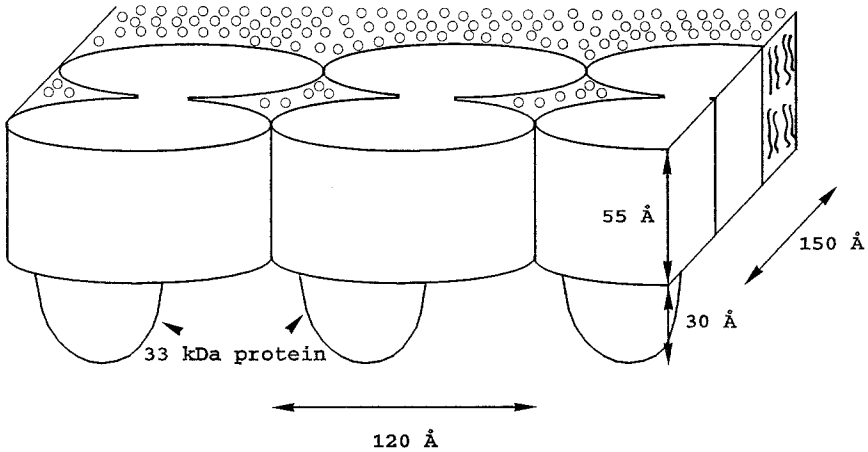

Fig. 10. A model for the structure of cyanobacterial PS II and its arrangement in the membranes (modified from Dekker *et al.*, 1988).

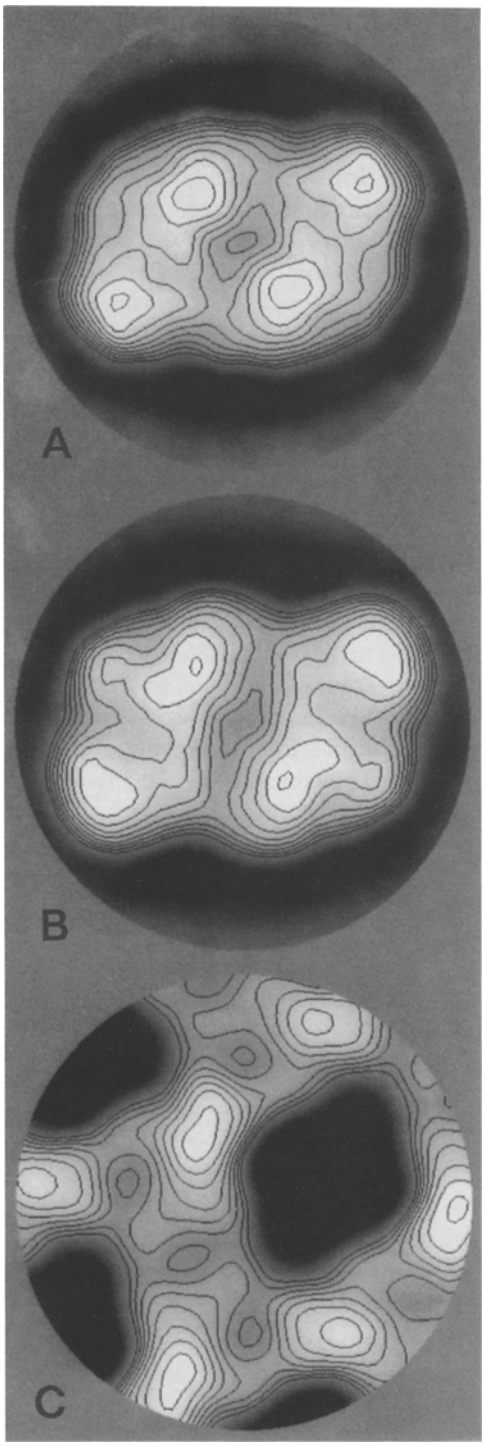

Fig. 11. Photosystem II from the thermophilic cyanobacterium *Synechococcus elongatus* and from spinach. (A) single-particle analysis of *Synechococcus* PS II dimers: an average view of 55 projections (Bald, Rögner, Boonstra, and Boekema, unpublished results). (B) single-particle analysis of spinach PS II dimers: an average view of 143 projections (Hankamer, Barber, Bald, Rögner, Boonstra, and Boekema, unpublished results). (C) spinach PS II monomers, analyzed from two-dimensional crystals (modified from Dekker *et al.*, 1990). The diameter of the circular mask is 228 Å. Note: two-fold symmetry was imposed on the images of A and B, because in the nonsymmetrized version the two-fold symmetry was obvious. This indicates that the two monomers are aranged in an antiparallel way in cyanobacteria and green plants.

green plant membranes (Miller and Cushman, 1978). If the subunits associated with oxygen evolving are removed from the membrane, the particles appear dimeric (Seibert *et al.*, 1987).

Evidence for the existence of a dimeric organization of PS II *in vivo* was obtained by free-fracturing (Mörschel and Schatz, 1987). The explanation for the dimeric character of PS II in cyanobacteria could be that each dimer serves as an anchor for the attachment of one phycobilisome, the large extrinsic light-harvesting antenna of cyanobacteria. A model for the linear arrangement of PS II dimers was proposed by Dekker *et al.* (1988), which is depicted in Fig. 10.

PHOTOSYSTEM II FROM SPINACH

Isolated spinach PS II monomers with and without oxygen-evolving capacity (Irrgang *et al.*, 1988; Haag *et al.*, 1990) were studied. Both types of particles gave single-particle projections with overall dimensions 153 × 106 Å in the plane. If corrected for detergent, the dimensions were 119 × 72 Å, similar to those of the cyanobacterial PS II monomer. A protrusion presumably formed by the 33-kDa protein was found to have a thickness of 15–33 Å. This would increase the total thickness of PS II from 58 to 73–91 Å (Haag *et al.*, 1990), which is similar to the 80 Å, determined for the cyanobacterial oxygen-evolving PS II dimers (Dekker *et al.*, 1988).

Recently, a data set of about 1000 projections from spinach PS II dimers could be investigated (Hankamer, Barber, Bald, Rögner, Boonstra, and Boekema, unpublished results). These dimers consist of the D1 and the D2 protein, the two small subunits of cytochrome b_{559}, and the 47-, 43-, and 33-kDa subunits, and lack peripheral light-harvesting antenna proteins. Image analysis revealed the features of these dimeric PS II particles. The overall maximal length and width, as determined from Fig. 11B, are about 197 and 135 Å, respectively. These dimensions differ somewhat from the 185 and 155 Å determined for *Synechococcus* PS II dimers (Rögner *et*

al., 1987) and the dimensions from Fig. 11A, which were 184 and 128 Å. However, at this stage it is not clear whether this discrepancy is due to real structural differences.

A comparison of the spinach dimers can be made with a smaller PS II particle lacking the 43-kDa subunit and the extrinsic 33-kDa subunit. This particle was studied from two-dimensional crystals (Dekker *et al.*, 1990). Comparison of the top views shows that the two PS II particles have some features in common (Fig. 11). Since the 33-kDa subunit is supposed to be outside of the membrane plane, the difference in size in the projection may largely be attributed to the 43-kDa subunit. Thus, it can be concluded that the 43-kDa subunit is located at the tip of the PS II monomer. By comparison of several dimers, all with a slightly different subunit composition, and by immunolabeling, it should be possible to localize the larger subunits within PS II.

Recently, a low-resolution three-dimensional model was calculated based on small negatively stained two-dimensional crystals from membrane-enriched PS II (Holzenburg *et al.*, 1993). The lumenal side of the PS II model is characterized by four dense domains surrounding a cavity. The features of this part of the protein and of our dimeric PS II projection are similar, suggesting that these four lumenal domains mainly originate from the large extrinsic loops of two CP47 and two CP43 apoproteins and from the 33-kDa extrinsic proteins. Most remarkably, the dimeric symmetry is fully absent on the stromal side. This led the authors to the conclusion that in fact the structure represents monomeric PS II. This would mean that within the dimer some subunits are present with only one copy. Larger two-dimensional crystals were grown by Lyon *et al.* (1993) and were analyzed to a resolution of 17 Å, but only in projection. The crystals consisted of two monomeric units arranged around a central cavity to form a dimer. At 17 Å resolution, tests showed that the two halves of the dimer were identical. Volume calculations suggested that each dimer consisted of two PS II complexes. In the analysis of our dimers we could also not find much deviation from the two-fold symmetry. Therefore we present Fig. 11A, B in the two-fold symmetrized form. Moreover, the spinach and cyanobacterial monomers show oxygen evolution, which indicates that they contain at least one copy of the 33-kDa subunit, plus D1, D2, and the 43- and 47-kDa proteins. Also, the shape of the monomer (Fig. 9B in Irrgang *et al.*, 1988) is similar to the shape of a 1/2 dimer in Fig. 11B. Thus, there is no reason to doubt the dimeric nature of PS II.

The PS II structure from Holzenburg *et al.* (1993) is maximally 190 × 168 Å. The maximal length and width of the spinach dimers are 163 × 100 Å, if dimensions are corrected for attached detergent. The different dimensions give some support for the proposal of Holzenburg *et al.* (1993) that light-harvesting chlorophyll *a/b* proteins are present in their PS II crystals. However, it is unlikely that all the light-harvesting chlorophyll *a/b* proteins associated with PS II would be present. There is evidence that the major one, the light-harvesting complex II (LHCII), occurs in trimers *in vivo* because the CD characteristics of monomeric LHCII are quite different from those observed in trimeric LHCII and in thylakoid membranes (S. B. Nussberger, W. Kühlbrandt, B. M. van Bolhuis, R. van Grondelle, J. P. Dekker, and H. van Amerongen, to be published). The LHCII trimers have a diameter of 75 Å (Kühlbrandt and Wang, 1991). Judging from the size of the crystals made by Holzenburg *et al.* (1993), it is unlikely that copies of such trimeric LHCII particles are present. This makes the 29-, 26-, and 24-kDa chlorophyll *a/b* proteins more likely candidates to be present.

CYTOCHROME *b6/f* COMPLEX

EM has been carried out recently on the cytochrome *b6/f* complex purified from the cyanobacterium *Synechocystis* PCC 6803. Negatively stained samples show elongated and rodlike projections which can be interpreted as top and side views of the particles (Fig. 12A). Image analysis of these projections, Fig. 12B, C, yield the dimensions of the averaged top view, 117 × 73 Å, and the averaged side view, 119 × 59 Å. The dimensions of the particle after correction for the contribution of the detergent are 83 × 44 × 60 Å (length × width × height). From these corrected dimensions a mass of about 70–130 kDa can be estimated, indicating that the complex is isolated as a monomer. This is in agreement with a mass estimation by gel filtration HPLC of 110 ± 20 kDa and an analysis of the subunit composition (Bald *et al.*, 1992). Due to the small size of this monomer, it cannot be expected that single-particle analysis will be of further help for elucidation of the structure. This may be possible, however, with

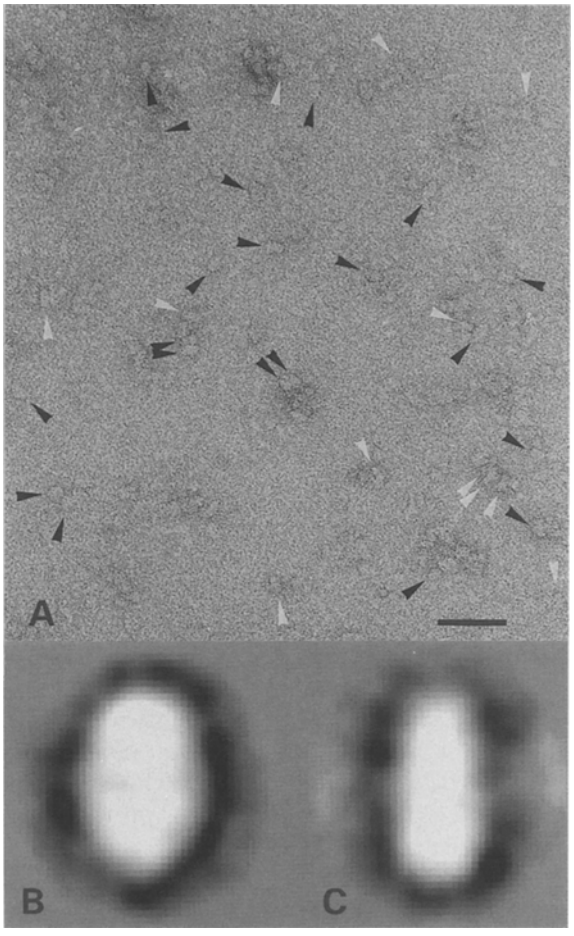

Fig. 12. Electron microscopy and image analysis on monomeric complexes of Cytochrome *b6/f* from the cyanobacterium *Synechocystis* PCC 6803. (A) electron micrograph of monomeric particles, negatively stained with 1% uranyl acetate. Top and side views are indicated by black and white arrows. The bar indicates 500 Å. (B) Average image of 70 top-view projections. (C) average image of 40 side-view projections.

two-dimensional crystals. Very recently, crystals have been obtained by Mosser, Dörr, Hauska, and Kühlbrandt from spinach Cytochrome *b6/f* (W. Kühlbrandt, personal communication).

FUTURE DIRECTIONS

The number of structures solved by X-ray diffraction or NMR at high resolution is steadily growing. Since 1990 nearly 400 new X-ray crystal structures and over 100 new NMR structures have been reported (Hendrickson and Wüthrich, 1993). The information on the low-resolution structure of large protein complexes by EM is also increasing. A recent development is the combination of X-ray structures with EM data. Especially for viruses, the fitting parts of a structure solved at high resolution (capsid proteins) into large structures determined at low resolution (viruses of several 100 Å in diameter) has been found useful (Smith *et al.*, 1993; Stewart *et al.*, 1993). It may be impossible to obtain atomic resolution for such complicated structures as the PS I, PS II, and the F_0F_1ATP synthase complex including their interacting donor, acceptor, and regulatory molecules and proteins in a short term. Meanwhile, a combination of EM reconstructions of these large photosynthetic membrane complexes with atomic structures of their individual components will become important for understanding the structure and function of these proteins.

ACKNOWLEDGMENTS

We thank Prof. E. F. J. van Bruggen for support, Dr. W. Keegstra for his help with computer image analysis, and Mr. K. Gilissen for photography. This work was supported by the Netherlands Foundation for Chemical Research (SON) with financial aid from the Netherlands Organization for Scientific Research (NWO). J. P. D. was supported by a grant from the Royal Netherlands Academy of Arts and Sciences (KNAW), and M. R. by a grant from the Deutsche Forschungsgemeinschaft (DFG) and a grant from the Northrhine Westfalian Ministry of Science and Research (Bennigsen-Foerder-Prize).

REFERENCES

Amzel, L. M., Bianchet, M. A., and Pedersen, P. L. (1992). *J. Bioenerg. Biomembr.* **24,** 429–433.

Bald, D., Kruip, J., Boekema, E. J., and Rögner, M. (1992). In *Current Research in Photosynthesis* (N. Murata, ed.), Kluwer, Dordrecht, Vol. 1, pp. 629–632.

Boekema, E. J. (1991). *Micron Microsc. Acta,* **22,** 361–369.

Boekema, E. J., Dekker, J. P., van Heel, M. G., Rögner, M., Saenger, W., Witt, I., and Witt, H. T. (1987). *FEBS Lett.* **217,** 283–286.

Boekema, E. J., Schmidt, G., Gräber, P., and Berden, J. A. (1988). *Z. Naturforsch.* **43C,** 219–225.

Boekema, E. J., Dekker, J. P., Rögner, M., Witt, I., Witt, H. T., and van Heel, M. G. (1989). *Biochim. Biophys. Acta* **974,** 81–87.

Boekema, E. J., Wynn, R. M., and Malkin, R. (1990). *Biochim. Biophys. Acta* **1017,** 49–56.

Boekema, E. J., Harris, D., Böttcher, B., and Gräber, P. (1992). In *Current Research in Photosynthesis* (N. Murata, ed.), Kluwer, Dordrecht, Vol. 2, pp. 645–652.

Böttcher, B., Gräber, P., and Boekema, E. J. (1992). *Biochim. Biophys. Acta* **1100,** 125–136.

Bryant, D. A. (1992). In *Topics in Photosynthesis, Vol. 11, The Photosystems: Structure, Function and Molecular Biology.* (Barber, J., ed.), Elsevier, Amsterdam, pp. 501–549.

Capaldi, R. A., Aggeler, R., Gogol, E. P., and Wilkens, S. (1992). *J. Bioenerg. Biomembr.* **24,** 435–439.

Chitnis, V. P., Xu, Q., Yu, L., Golbeck, J. H., Nakamoto, H., Xie, D-.L., and Chitnis, P. R. (1993). *J. Biol. Chem.* **268,** 11678–11684.

Dainese, P., Santini, C., Ghiretti-Magaldi, A., Marquardt, J., Tidu, V., Mauro, S., Bergantino, E., and Bassi, R. (1992). In *Research in Photosynthesis* (Murata, N., ed.), Kluwer, Dordrecht, Vol. 2, pp. 13–20.

Dekker, J. P., Boekema, E. J., Witt, H. T., and Rögner, M. (1988). *Biochim. Biophys. Acta* **936,** 307–318.

Dekker, J. P., Betts, S. D., Yocum, C. F., and Boekema, E. J. (1990). *Biochemistry* **29,** 3220–3225.

Erickson, J. M., and Rochaix, J. D. (1992). In *Topics in Photosynthesis, Vol. 11, The Photosystems: Structure, Function and Molecular Biology* (Barber, J., ed.), Elsevier, Amsterdam, pp. 101–172.

Ford, R. C., Hefti, A., and Engel, A. (1990). *EMBO J.* **9,** 3067–3075.

Frank, J., Radermacher, M., Wagenknecht, T., and Verschoor, A. (1988). *Methods Enzymol.* **164,** 3–35.

Haag, E., Boekema, E. J., Irrgang, K. D., and Renger, G. (1990). *Eur. J. Biochem.* **189,** 47–63.

Haley, J., and Bogorad, L. (1989). *Proc. Natl. Acad. Sci. USA* **86,** 1534–1538.

Henderson, R., Baldwin, J. M., Ceska, T. A., Zemlin, F., Beckmann, E., and Downing, K. H. (1990). *J. Mol. Biol.* **213,** 899–920.

Hendrickson, W. A., and Wüthrich, K. (eds.) (1993). *Macromolecular Structures 1993*, Current Biology, London.

Holzenburg, A., Bewley, M. C., Wilson, F. H., Nicholson, W. V., and Ford, R. C. (1993). *Nature (London)* **363,** 470–473.

Ikeuchi, M. (1992). *Plant Cell Physiol.* **33,** 669–676.

Irrgang, K.-D., Boekema, E. J., Vater, J., and Renger, G. (1988). *Eur. J. Biochem.* **178,** 209–217.

Krauss, N., Hinrichs, W., Witt, I., Fromme, P., Pritzkow, W., Dauter, Z., Betzel, C., Wilson, K. S., Witt, H. T., and Saenger, W. (1993). *Nature (London)* **361,** 326–331.

Kruip, J., Boekema, E. J., Bald, D., Boonstra, A. F., and Rögner, M. (1993). *J. Biol. Chem.*, in press.

Kühlbrandt, W., and Wang, D. N. (1991). *Nature (London)* **350,** 130–134.

Lyon, M. K., Marr, K. M., and Furcinitty, P. S. (1993). *J. Struct. Biol.* **110,** 133–140.

Miller, K. R., and Cushman, R. A. (1978). *Biochim. Biophys. Acta* **546,** 481–499.

Mörschel, E., and Schatz, G. H. (1987). *Planta* **172,** 145–154.

O'keefe, D. P. (1988). *Photosynth. Res.* **17,** 189–216.

Rögner, M., Dekker, J. P., Boekema, E. J., and Witt, H. T. (1987). *FEBS Lett.* **219,** 207–211.

Rögner, M., Mühlenhoff, U., Boekema, E. J., and Witt, H. T. (1990). *Biochim. Biophys. Acta* **1015,** 415–424.

Schuster, G., Nechustai, R., Ferreira, C.G., Thornber, J.P., and Ohad, I. (1988). *Eur. J. Biochem.* **177,** 411–416.

Schwartz, E., Shen, D., Aebersold, R., McGrath, J. M., Pichersky, E., and Green, B. (1991). *FEBS Lett.* **280,** 229–234.

Seibert, M., DeWit, M., and Staehelin, L. A. (1987). *J. Cell Biol.* **105,** 2257–2265.

Smith, T. J., Olson, N. H., Cheng, R. H., Liu, H., Chase, E. S., Lee, W. M., Leippe, D. M., Mosser, A. G., Rueckert, R. R., and Baker, T. S. (1993). *J. Virol.* **67,** 1148–1158.

Staehelin (1988). In *Photosynthesis III* (Staehelin, L. A., and Arntzen, C. J., eds.), Springer, Berlin, pp. 1–84.

Stewart, P. L., Fuller, S. D., and Burnett, R. M. (1993). *EMBO J.* **12,** 2589–2599.

Svensson, B., Vass, I., Cedergren, E., and Styring, S. (1990). *EMBO J.* **9,** 2051–2059.

Van der Staay, G. W. M., Boekema, E. J., Dekker, J. P., and Matthijs, H. C. P. (1993). *Biochim. Biophys. Acta* **1142,** 189–193.